

Acoustic monitoring of the gelation of a colloidal suspension

Nicolas Bécicard, Marc Junior Niémet-Mabiala, Jean-Noel Tourvieille, and Pierre Lidon

Univ. Bordeaux, CNRS, Solvay, LOF, Pessac, F-33600, France

(*pierre.lidon@u-bordeaux.fr)

(*jean-noel.tourvieille@solvay.com)

(*nicolas.belicard@gmail.com)

(Dated: January 19, 2022)

Because they are sensitive to mechanical properties of materials and can propagate even in opaque systems, acoustic waves provides us with a powerful characterization tool in numerous fields. Common techniques mostly rely on time-of-flight measurements and do not exploit the spectral content: however, sound speed and attenuation spectra contain rich information. Such an acoustic spectroscopy already exists and allows to retrieve subtle information on systems of well-known physico-chemistry, but modeling becomes out of reach for industrial systems. In this article, we use a simple empirical approach to monitor the gelation of silica suspensions: we show that the gelation time obtained from acoustic measurements is proportional to this determined with more conventional rheological characterization. Such a results thus opens the way for in-situ monitoring of time-evolving systems in industrial context with acoustic methods only.

I. INTRODUCTION

Acoustic waves are coupled perturbation of deformation and pressure propagating across any medium (even opaque), that can be longitudinal (associated with compression) or transverse (associated with shear deformations, strongly damped in liquids). They are thus sensitive to mechanical properties of materials. Acoustic methods can consequently be alternative or complementary to their optical counterparts.

In particular, acoustic imaging and velocimetry techniques have been developed and significantly improved in the last decades, providing us with powerful tools for characterization of opaque systems [1–4]. High-frequency ultrasonic waves are indeed associated with short wavelength (typically of a few 100 μm for frequency around 10MHz in water, and smaller in solid materials) and consequently offer a satisfactory spatial resolution in many situations. They rely essentially on the measurement of the time-of-flight of acoustic echoes generated by the reactions of an initial pulse on interfaces or defects in heterogeneous media, or on tracer particles in systems under flow. Together with the development of versatile and low cost piezoelectric transducers, this explains the large success of ultrasonic imaging and velocimetry in biomedical application or in non-destructive testing of materials in field situations, where optical imaging is not possible due to opacity. However, they require costly electronic devices and heavy signal analysis which impedes their use in physico-chemical characterization.

These methods are mostly based on the measurement of sound speed: however, acoustic attenuation also contains rich information. In homogeneous liquids, heat conduction effects on sound propagation are negligible and attenuation is mostly determined by shear viscosity, bulk viscosity (which is due to compressibility effects and is correlated with shear viscosity, but not always linearly) and possible relaxation phenomena between molecular energy levels [5, 6]. If no microscopic relaxation occurs in the probed frequency range, simple measurement of acoustic attenuation can be used as a proxy for viscosity in industrial systems [7, 8]. However, measurements of full attenuation spectra are preferable to avoid artifacts [9]:

such an acoustic spectroscopy technique has been developed leading to commercial apparatuses to measure viscoelastic moduli at frequencies far above the range accessible to conventional rheometers [10–14]. In systems of well controlled physico-chemistry, modeling of acoustic attenuation accounting for relaxation phenomena gives access to subtle information on microscopic dynamics [15, 16].

In heterogeneous systems, interpretation of acoustic spectra is more complex and remains an open question. In controlled suspensions, measured attenuations [17–19] can be described by rigorous yet sophisticated models [20–26] or by more empirical approaches [27, 28] but such modeling is still out of reach for more complex industrial systems. For instance, some studies were devoted to sound attenuation in biomedical [29–31], pharmaceutical [32, 33] or food samples [34–37], but they remain mostly qualitative and do not attempt to model acoustic signals.

However, acoustic spectroscopy remains interesting for monitoring evolving physico-chemical systems, by following a more empirical approach. In this case, it is sufficient to quantify a correlation between ultrasound spectroscopic measurements and another established characterization technique to later use acoustic spectroscopy autonomously. Rheometry is relevant for this correlation as it is sensitive to similar properties. Such an approach has been followed in particular for the monitoring of food science processes [35–37] or of chemical gelation [38–40] for instance.

Colloidal gels form due to the growth of a rigid network of solid particles: such a process is likely to impact significantly sound propagation. Surprisingly, acoustic studies of such gelation are scarce and existing works did not correlate acoustic measurements with another technique and therefore remained essentially qualitative [41]. In this paper, we propose a simple setup of ultrasound spectroscopy and use it to monitor the gelation kinetics of a silica colloidal suspension destabilized by the addition of a brine, a system that has been previously studied by various optical and rheological techniques [42–44]. By analyzing transmitted and reflected acoustic pulses across a home-built measurement cell of controlled temperature, we measure sound speed and attenuation spec-

tra during the whole gelation process. We show that attenuation progressively increases at all frequencies and allows us to define a characteristic gelation time. This time is compared to gelation time measured from viscoelastic moduli obtained by rheometry: we prove that the two times, if not equal, are proportional to each other and of similar order of magnitude which opens possibilities for monitoring of gelation by acoustical means only.

In Section 2, we first introduce the materials and methods used in this work: in particular, we present the acoustic setup and the principles of signal analysis to obtain acoustic spectra. The rheological and acoustic results are then presented and compared in Section 3. In Section 4, we finally discuss opportunities and limitations in our setup: in particular, we show that a more precise analysis of acoustic spectra can reveal properties of the gel and that it is possible with our setup to map spatially the properties of the gel.

II. MATERIALS AND METHODS

A. Formulation of Ludox gels

In this work, we focus on the same type of gel as in the studies by Trompette et al. [42, 43, 45, 46] and by Cao et al. [44] that served as a guide for formulation. For all experiments, we used an initial suspension of silica nanoparticles (Ludox HS-40, Sigma Aldrich) with a 40%wt. content of solid and average particle radius 6 nm as specified by the manufacturer. The solution is mixed with a brine made of sodium chloride (NaCl) salt dissolved in deionized water. In order to modify gelation kinetics, we modified the brine concentration between 0.35 molL^{-1} and 0.65 molL^{-1} while keeping a similar volume fraction $\phi = 5.9\%$ of Ludox particles (assuming a density of $\rho = 1.3 \text{ kg m}^{-3}$ for the initial suspension, as indicated by the supplier) in the final gel.

Physico-chemical properties of Ludox silica colloidal suspensions are complex [46, 47] but can be qualitatively described by the main elements of DLVO theory. In the initial suspension, the negative surface charge of particles induces a dominant electrostatic repulsion which stabilizes the solution. When mixed with brine, salts in solution screen this surface charge and attractive van der Waals interaction dominates the interaction potential, leading to a progressive agglomeration of colloids. A fractal network of particles forms and grows in time, giving elastic properties to the gel when it percolates across the sample.

Both for acoustical and rheological measurements, the experimental cell is maintained at a constant temperature $T = (23.0 \pm 0.1)^\circ\text{C}$ and the brine and Ludox suspensions are initially thermalized at the same temperature, in order to limit temperature transients. The two solutions are vigorously introduced in the measuring cell to favor an initial homogeneous mixing which sets the origin of time $t = 0$ in the experiments. The solution progressively turns into a gel, which can be visually observed by it becoming opalescent due to the growth of the colloidal network. The volume fraction of Ludox and concentration of the brine were chosen to keep a gelation time

long enough to allow for loading and thermalization of the sample, while being short enough to ensure experiments run over less than one day.

B. Rheological measurements

In order to have a basis for interpretation of acoustic signals, we performed rheological characterizations by measuring the evolution of the viscoelastic moduli over the gelation process. Experiments are done in a sand-blasted cylindrical Couette geometry (inner radius 25 mm, gap 2.5 mm) with a stress-controlled rheometer (Malvern Kinexus Extra+), at controlled temperature $T = 23^\circ\text{C}$.

After loading the suspension and the brine, we monitor the evolution over time of the viscoelastic moduli at an imposed shear amplitude of $\gamma = 0.1\%$, in order to minimally disturb the gelation process and remain in the linear rheological domain after gelation for all probed frequencies. Gelation is slow enough so we can perform measurements at different frequencies: rheometer repeats over time seven steps of frequencies ranging from 0.1 Hz to 1 Hz.

C. Acoustic setup and measurements

1. Setup

The setup is depicted on Fig. 1. Two piezoelectric immersion transducers (Olympus V312-SU, central frequency 10 MHz, bandwidth 4 – 12 MHz, diameter 6 mm) were placed on both sides of the sample, in a small water tank in order to maximize acoustic transmission. One transducer is connected to a pulse generator (Sofranel DPR300) which generates short electrical impulses (duration around $0.5 \mu\text{s}$) with a tunable repetition rate in order to create acoustic pulses. Our setup allows for two different measurements: the emitting transducer can also be used as a receiver to measure reflected signals while the other transducer is used to acquire transmitted signals. The earlier was connected to an amplification and filtering stage included in the pulse generator, and both are eventually linked to an oscilloscope (Keysight InfiniiVision 2000X) triggered by the pulse generator for data acquisition and digitization. In order to improve the signal-noise ratio, measurements were averaged over ten pulses with a pulse repetition frequency of 1 Hz to ensure a good separation between successive pulses: given the slow evolution of the gel and the high accessible pulse repetition frequency, this does not limit significantly the time resolution of our setup.

Temperature is known to influence acoustic measurements and in particular sound speed: we thus took great care to ensure the sample under study was kept under isothermal conditions to avoid any thermal bias. To this purpose, the sample was placed in a triple-walled cell built in a resin by a SLA 3D printer (Formlabs, High Temp resin). The triple wall allowed circulation of water whose temperature is imposed by a thermal bath driven by a feedback loop controlled by a platinum resistance thermometer (4 point PT100, Radiospares)

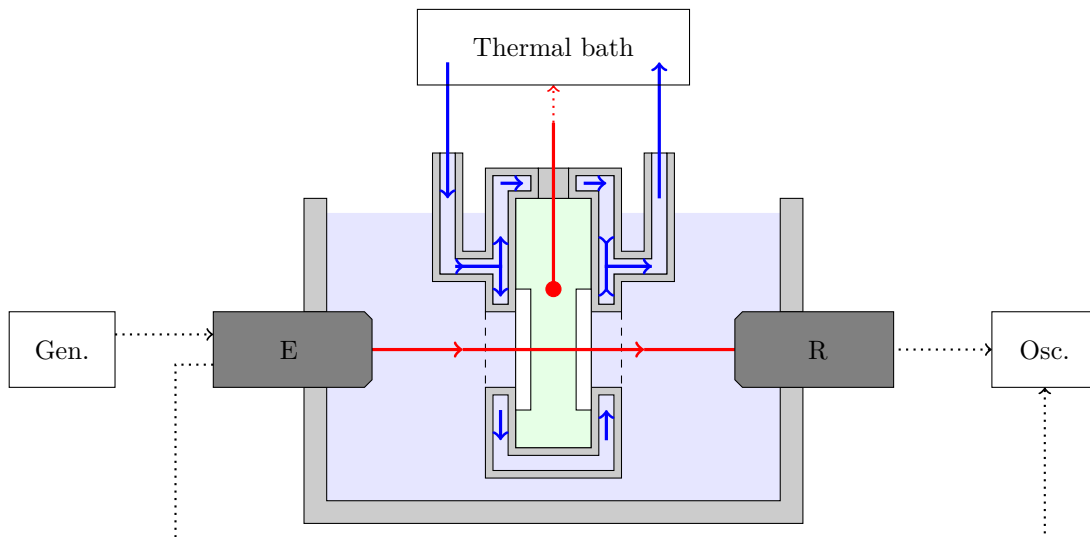


FIG. 1. Schematics of the acoustic setup. The sample under study (in green) is placed in a double walled cell, allowing inner water circulation (blue arrows) to control the temperature through a feedback loop driven by a thermometer plunged in the sample. The cell is closed by polycarbonate windows (in white) to allow ultrasound propagation. Acoustic transducers (dark gray) are placed and aligned on both sides of the cell. The emitting transducer E is powered by a pulse generator (Gen.) and is also used to acquire reflected signals. The receiving transducer T is used to collect transmitted signals. Both signals are digitized by an oscilloscope (Osc.). The acoustic path is materialized by the red line.

plunged inside the sample. This setup allowed to reduce temperature fluctuations below 0.1 °C after typical thermalization transients of a few minutes.

In order to limit interfaces on the acoustic path, the cell wall was designed with a small opening on both sides which is closed by a polycarbonate window (in white on Fig. 1) of homogeneous thickness about 1 mm. This window is isotropic and homogeneous for ultrasound propagation which simplifies the analysis of acoustic signal.

Finally, the setup requires some alignment steps: to this purpose, the measurement cell is held by a ball joint on translation platforms in order to control both its orientation and position. First, the two transducers are aligned parallel and along the same axis by maximizing the amplitude of the transmitted signal. Then, the cell is placed in between and aligned with windows orthogonal to the acoustic propagation direction by maximizing the amplitude of the signal reflected by the first window.

2. Signal analysis

We assume that acoustic signals can be described by unidimensional wave packets in our setup. The acoustic pressure at position x and time t for a single freely propagating pulse can then be written as:

$$u(x, t) = \int u_{\omega}^0 e^{j[k(\omega)x - \omega t]} d\omega \equiv \int u_{\omega}(x) e^{-j\omega t} d\omega \quad (1)$$

where u_{ω}^0 represents the spectral content of the source and u_{ω} is the Fourier transform of the signal. The wave vector $k(\omega) = k'(\omega) + jk''(\omega)$ is a complex number, and its value

for a given frequency is set by the properties of the material through a dispersion relation. One can define the (frequency-dependent) sound speed c_{ω} and attenuation coefficient α_{ω} by setting $k' = \omega/c_{\omega}$ and $k'' = \alpha_{\omega}$. The Fourier transform of the wave packet can then be expressed as

$$u_{\omega}(x) = u_{\omega}^0 e^{j\omega x/c_{\omega}} e^{-\alpha_{\omega} x}. \quad (2)$$

For propagation across a distance ℓ of a wave at pulsation ω , the time of flight is given by $\tau_{\omega} = \ell/c_{\omega}$ and the attenuation factor is $e^{-\alpha_{\omega} \ell}$. We note that the attenuation α is expressed in Neper per meter (Np/m), expressing that it is obtained with a Neper logarithm from attenuation factor (by opposition with the decibel which is also commonly used, which is obtained with a decimal logarithm).

When a wave packet crosses an interface, it generates a transmitted and a reflected echo of proportional amplitudes, that later propagates towards the next interface. In our setup, the two transducers allowed us to record these successive echoes generated by the initial pulse during its propagation in the water tank, in the windows of the cell and in the sample of interest. The time of flights and attenuation of these pulses are thus not only related to the sample, but also to the propagation in the rest of the setup: obtaining absolute measurements is not possible with our current experiment. We can however obtain relative values with respect to a reference medium, chosen as water because its acoustic properties are precisely known.

The calibration procedure is described in details in Appendix A. Shortly, we normalized our measurements by reference signals obtained by reflection on a cell filled with air (the air/window interface being perfectly reflecting for acoustic waves) and by reflection on and transmission through a cell

filled with water. This allowed us to obtain the reflection and transmission coefficients of the various interfaces and to factor out the effects of propagation through other media. We finally obtained the excess time of flight and excess attenuation for the propagation across the length ℓ of sample, compared to the propagation across a similar length of water. As the length ℓ is also calibrated, and by using tabulated acoustic properties of water [48, 49], we can deduce the sound speed and attenuation of the sample.

III. EXPERIMENTAL RESULTS

A. Gelation time(s) from rheological measurements

The evolution of the viscoelastic moduli G' and G'' after mixing the brine and the colloidal suspension are presented in Fig. 2, for different brine concentrations. The overall evolution is consistent with results reported by Cao et al. [44]. First, both moduli are very small and at the limit of resolution of the rheometer. After a time delay τ_d , there is a sudden rise of both moduli, which is followed by a more progressive increase while the gel ages. For some samples, we observe sudden drops of the elastic modulus when the system is gelified: we suspect that this is due to wall slip events, despite the walls of the geometry were sandblasted. As they happen after gelation, these events do not affect significantly our measurements of gelation time. Moreover, we will mostly focus on measurements obtained from the viscous modulus G'' that does not show these drops, as it is more directly related to acoustic attenuation.

In order to check for reproducibility, we repeated some of the formulations: we observe that despite some variability in the absolute values of the moduli (particularly visible on their final values), there is still a clear difference of dynamics when varying the amount of salt in the system, more concentrated brine leading to faster gelation. However, it is to note that the least concentrated sample (for $[\text{NaCl}] = 0.35 \text{ mol L}^{-1}$) hardly started to gelify at the end of the experiment: it is thus dubious to interpret results for this gel. We will present our measurement for this gel on figures, but it will be excluded for fittings.

In order to quantify the dynamics of gel formation, we need to define a gelation time. Different options are possible from rheological measurements. For all the different definitions presented in the following, the relative variation of gelation time obtained when reproducing the experiment in the same conditions is about 10%, which is taken as the associated uncertainty.

The most rigorous definition is given by the Winter criterion: by analyzing the evolution in time of the viscoelastic moduli at different frequencies, the gelation time τ_W can be defined as the time at which the loss angle $\tan \delta = G''/G'$ is independent of frequency. This criterion was justified by theoretical arguments on the behavior of viscous and elastic moduli when approaching the critical point of percolation [50–54]. It also coincides approximately with the time at which the elastic modulus G' overcomes the viscous one G'' [55, 56], which is a more intuitive definition. While being initially in-

troducted for chemical gels forming by reticulation, this criterion has also been successfully applied to the physical gels we are investigating [45].

The times obtained from Winter criterion for different brine concentrations are plotted on Fig. 3(a). In agreement with measurements of Cao et al. [44], they evolve exponentially with concentration $[\text{NaCl}]$ along:

$$\tau_W = \tau_{0,W} e^{-\kappa_W [\text{NaCl}]} \quad (3)$$

with $\tau_{0,W} \simeq 3.6 \times 10^5 \text{ s}$ and $\kappa_W = (8.5 \pm 0.5) \text{ L mol}^{-1}$. We remind the reader that we excluded the least concentrated sample from this fit, as it did not reach a complete gelation at the end of the experiment and the $\tan \delta$ curve do not intersect very clearly. It is interesting to note that the coefficient κ we obtain is in agreement with the value obtained in the literature $\kappa_{\text{itt}} = (8.3 \pm 1.2) \text{ L mol}^{-1}$ for similar gels [44].

However, Winter criterion is not very convenient to use. First, it was difficult with some samples to observe a clear crossing of the $\tan \delta$ curves at different frequencies. Moreover, these measurements are long to perform as they require to be made at different frequencies. It is thus interesting to define gelation times by other means. A simple criterion is obtained by measuring the delay time τ_d at which the viscoelastic moduli start rising: the obtained results are displayed on Fig. 3(b). We observe that the times obtained by analyzing the elastic and viscous moduli are similar: consequently, we will mostly focus on the times obtained from G'' , as they are more likely to be correlated with the acoustic attenuation that will be exploited in section III B. Moreover, it also follows an exponential evolution (3), with a typical time $\tau_{0,d} \simeq 1.1 \times 10^6 \text{ s}$ and concentration $\kappa_d = (10.4 \pm 0.5) \text{ L mol}^{-1}$. This value of κ remains close to this obtained previously, which suggests the delay time is also a good marker of gelation.

Finally, we tested other ways to define a gelation time. It is easy to measure a time of rise at 63% of the final value for G' and G'' : the results are rather similar and also evolve exponentially with brine concentration $[\text{NaCl}]$. We also tried to fit the evolution of both moduli with a stretched exponential:

$$G(t) = G_\infty \left[1 - \exp \left[-\alpha \left(\frac{t}{\tau} - 1 \right)^\beta \right] \right]. \quad (4)$$

Such a function has been proposed by Cao et al. [44] for the elastic modulus but it also provides a satisfactory description of the viscous modulus. The obtained times from G' and G'' are close yet noticeably distinct, but they both still follow Eq. (3). For the sake of concision, we will discuss these other definitions in more details, but our conclusions remain similar with the other choices discussed here.

B. Gelation time from acoustic measurements

We reproduced the same formulations studied with the rheometer and monitored their gelation with the acoustic setup presented in Section II C. An example of evolution of average sound speed c and attenuation α is displayed on Fig. 4. The

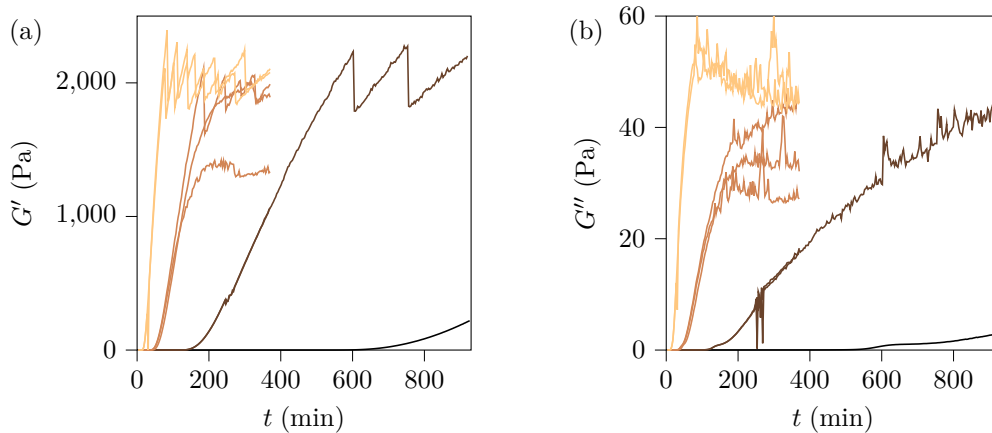


FIG. 2. Evolution of the elastic (a) and viscous (b) moduli at frequency $f = 1$ Hz and shear amplitude $\gamma = 0.1$ % during the gelation. For all samples, the volume fraction of particles is $\phi = 5.9$ %. Lighter colors correspond to more concentrated brines, and brine concentrations are respectively $[\text{NaCl}] = 0.35, 0.45, 0.55$ and 0.65 molL^{-1} .

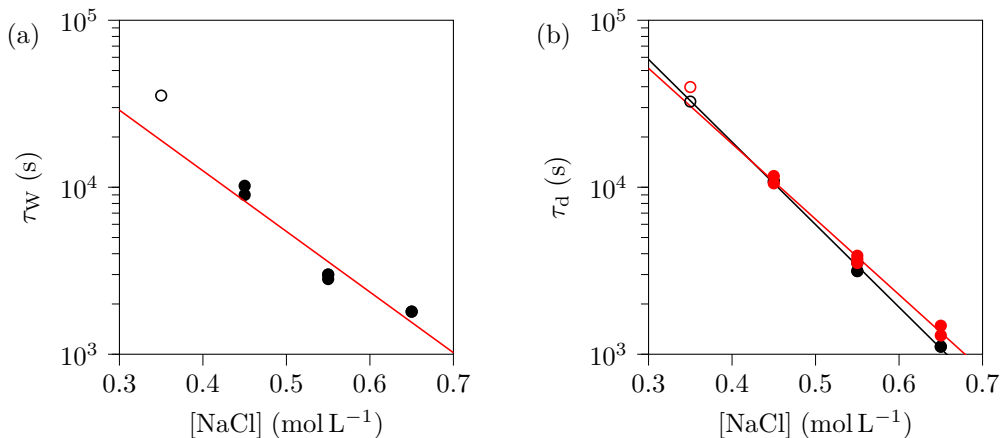


FIG. 3. (a) Gelation time obtained from Winter criterion for varying brine concentrations. Red line displays an exponential fit along Eq. (3) with $\tau_{0,W} \simeq 3.6 \times 10^5 \text{ s}$ and $\kappa_W = (8.5 \pm 0.5) \text{ L mol}^{-1}$. (b) Gelation time obtained from the sudden rise of elastic (black symbols) and viscous (red symbols) moduli for varying brine concentrations. Lines correspond to an exponential fit along Eq. (3) with $\tau_{0,d} \simeq 1.8 \times 10^6 \text{ s}$ and $\kappa_d = (11.4 \pm 0.5) \text{ L mol}^{-1}$ (black line), and $\tau_{0,d} \simeq 1.1 \times 10^6 \text{ s}$ and $\kappa_d = (10.4 \pm 0.5) \text{ L mol}^{-1}$ (red line). In all fits, the point at $[\text{NaCl}] = 0.35 \text{ molL}^{-1}$ (open symbol) has been excluded.

grayed area represents the duration of the thermal transient over which the system temperature reaches the imposed value.

We observe that sound speed does not vary significantly over the duration of the experiment. This is probably due to the fact that it is dominated by the solvent compressibility, which does not evolve during gelation. The tiny remaining evolution (overall increase observed in this example) is not reproducible from one experiment to another and probably reflects some very local changes in the gel. We consequently will not exploit data from sound speed in the following. On the contrary, the attenuation displays a reproducible and progressive increase during the gelation process.

This evolution for the different samples is plotted on Fig. 5. We observe that, despite some variability, attenuation overall increases in time and is faster for higher brine concentrations: this qualitative observation is consistent with the aforemen-

tioned literature on Ludox gels [42–44] and our own rheological measurements of III A. This is also consistent with the fact that acoustic attenuation is somehow related to dissipation in the material, thus to the viscous modulus G'' . As in our rheological experiments, the sample at brine concentration $[\text{NaCl}] = 0.35 \text{ molL}^{-1}$ did not fully gelify over the duration of the experiment: we will display the associated result but exclude it from fit.

In order to compare our results with rheometrical characterization, we need to define a typical gelation time τ_{US} from the acoustic measurements. Here, there is no apparent delay in the evolution of α and noise in our data makes difficult to obtain a rising time at a given percent of the final value. Instead of smoothing the obtained curves, we fit the evolution

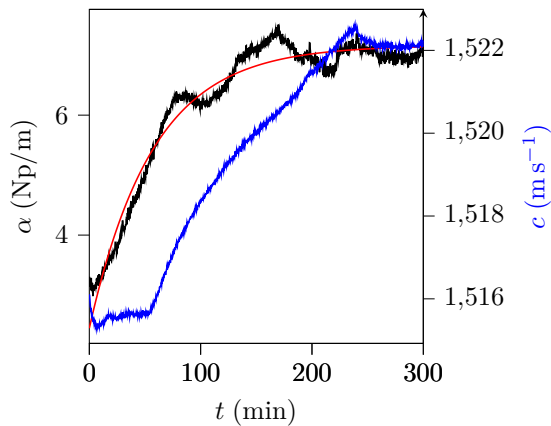


FIG. 4. Example of the acoustic attenuation α (black curve, left axis) and sound speed (blue curve, right axis) evolution during the gelation of a gel, with initial brine concentration $[\text{NaCl}] = 0.55 \text{ mol L}^{-1}$. The red curve corresponds to an exponential fit of the attenuation α according to Eq. (5) with $\Delta\alpha = 4.7 \text{ Np/m}$, $\alpha_0 = 2.4 \text{ Np/m}$ and $\tau_{\text{US}} = 3.4 \times 10^3 \text{ s}$. The gray area highlights the transient during which the sample is not thermalized.

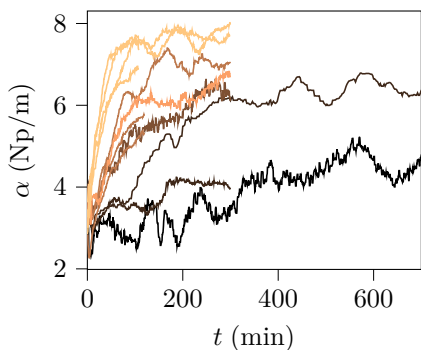


FIG. 5. Evolution of the acoustic attenuation α in time, for gels with identical particle volume fraction $\phi = 5.9\%$ and varying salt concentration $[\text{NaCl}] = 0.35, 0.4, 0.45, 0.50, 0.55$ and 0.60 mol L^{-1} . Lighter colors correspond to more concentrated brines.

by a generic exponential function:

$$\alpha(t) = \alpha_0 + \Delta\alpha \left(1 - e^{-t/\tau_{\text{US}}}\right). \quad (5)$$

Such an evolution describes satisfactorily the evolution of attenuation, as shown in Fig. 4, and the resulting gelation times are plotted for varying brine concentration in Fig. 6. By reproducing the experiment, typical relative variations of τ_{US} are of about 20%.

The evolution of gelation time again follows an exponential evolution with brine concentration, given by Eq. (3) with $\tau_{0,\text{US}} \simeq 8.4 \times 10^5 \text{ s}$ and $\kappa_{\text{US}} = (9.5 \pm 0.8) \text{ L mol}^{-1}$.

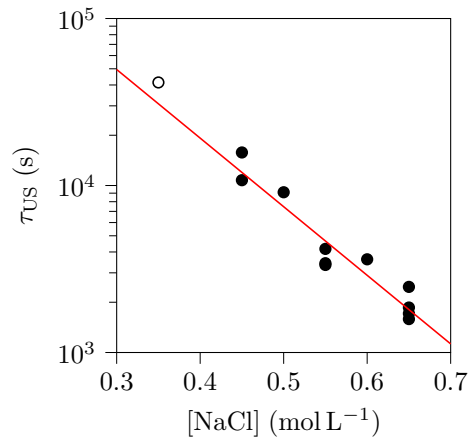


FIG. 6. Gelation time obtained from exponential fit of acoustic attenuation over time, for varying salt concentrations. The red line displays an exponential fit along Eq. (3) with $\tau_{0,\text{US}} \simeq 8.4 \times 10^5 \text{ s}$ and $\kappa_{\text{US}} = (9.5 \pm 0.8) \text{ L mol}^{-1}$. The open symbol corresponds to the sample at $[\text{NaCl}] = 0.35 \text{ mol L}^{-1}$ that did not fully gelify over the experiment duration and is excluded from the fit.

IV. DISCUSSION

A. Perspectives for monitoring of gelation processes

As presented in section III A and III B, the gelation times τ_{W} or τ_{d} obtained from conventional rheological measurements and τ_{US} from acoustic measurement evolve exponentially with salt concentration with a similar characteristic concentration $1/\kappa$. This shows that these times are all proportional which suggests that they all characterize gelation kinetics. This is not surprising that their values are not the same. First, the length scales that are probed by acoustics are not different: while the rheological characterization is sensitive to the apparition of elasticity at the length scale of the rheometer gap, acoustic measurement is more local. It is interesting to note that gelation time obtained from Winter criterion, which relies on a microscopic description of the gel structure, is of the same order of magnitude as the acoustic gelation time. Moreover, the mechanical sollicitation of the rheometer is pure shear while in acoustics, it also involves compression. Finally, even if shear amplitude in the rheometer is kept as small as possible, it is likely to disturb the gelation process by inducing some flow in the initial liquid state while ultrasound amplitude is too small to affect gelation [57].

This good correlation of gelation times opens the way to a purely acoustic monitoring of gelation, of interest in industrial context as it is a non-invasive method that can easily be adapted to inline processes. In particular, there is no need for modeling of the acoustic attenuation as we used a very generic exponential fitting. It is also interesting to note in another perspective that using focused transducers would allow to characterize smaller volumes of material, which is also interesting when comparing to conventional rheometry.

In our setup, we took great care to ensure isothermal conditions, which would be a major shortcoming for practical appli-

cations. However, this was required in order to minimize thermal biases for validation of the method. While sound speed is known to depend strongly on temperature, acoustic attenuation is only mildly affected by temperature fluctuations and a qualitative monitoring of gelation does not require the strict temperature control we employed in this experiment.

B. Analysis of acoustic spectra

In paragraph III B, we focused on the sound speed and attenuation averaged over the whole frequency range: however, our setup gives us access to the whole spectrum of these quantities and thus contains more information. An example of the evolution of the acoustic spectra during the gelation is presented in Fig. 7. A more complete representation can be obtained with colormaps in the time-frequency plane, as presented in Fig. 8.

We observe that there is no significant acoustic dispersion in the gel as the sound speed spectrum remains essentially flat over the whole transformation. However, the acoustic attenuation increases with frequency: as this evolution is monotonous, the average remains representative of the overall transformation but information is lost in the process.

Gaining more insights about the system from acoustic spectra requires modeling of acoustic attenuation. Describing acoustic propagation in colloidal gels is beyond our reach and we attempt a more phenomenological approach. Sound attenuation in a viscoelastic medium can be shown to be quadratic in frequency [58] following:

$$\alpha = \sqrt{\frac{\rho}{E}} \eta \omega^2 \quad (6)$$

where ρ is the density of the material, E is the elastic compressibility modulus and η corresponds to viscous dissipation (due to both regular shear viscosity and second viscosity which is due to compressibility effects). We thus focus on the rescaled attenuation $\varphi(\omega) = \alpha/\omega^2$, which is displayed on Fig. 9. This rescaling dampens a significant part of the variations of attenuation with frequency: we observe that the average value of φ increases in time, which implies that the effect on attenuation of viscous dissipation increases more than this of elasticity. Since the coefficients involved in α do not directly correspond to the viscoelastic moduli, there is no contradiction with rheological observations.

However, φ still displays variations with frequency. Such variations could be due to relaxation phenomena resulting from the interaction between the acoustic wave and the rigid skeleton of the gel. If we assume this relaxation is governed by a single time scale θ , the attenuation should become [5, 59–61]:

$$\alpha = A\omega^2 + B \frac{(\omega\theta)^2}{1 + (\omega\theta)^2} \quad (7)$$

which corresponds to a lorentzian profile of $\varphi(\omega)$, which would display an inflection point for a frequency $\omega^* = 1/(\sqrt{3}\theta)$. As showed on Fig. 9(b), this inflection indeed exists

for a frequency which is roughly constant in time, corresponding to a typical time $\theta = 1.1 \times 10^{-8}$ s. However, fitting $\varphi(\omega)$ with a lorentzian gives poor results, in particular it systematically results in negative values for parameter A .

For the varying brine concentration, the results remain qualitatively similar: sound speed, despite showing tiny and erratic variations in time, is independent on frequency, and attenuation increases with spectra roughly scaling like ω^2 . The observation of an inflection point of $\varphi(\omega)$ is in general observable, despite some irregularities of the spectrum quality, and the value of the relaxation time θ seems independent of the concentration of salt.

Other models for attenuation spectrum than the proposed relaxation (7) exist. For instance, a powerlaw attenuation $\alpha = \alpha_0 \omega^\gamma$ corresponding to a fractional Kelvin-Voigt model [62]) provides a better description of the spectra, but the evolution in time of the resulting parameters α_0 and γ show a poor reproducibility, even for similar formulations. At this stage, it is thus not possible to draw clear conclusions about the acoustic spectra. These results therefore remain preliminary and improved experimental data would be helpful, in particular with an extended frequency range to better constrain fits.

C. Mapping of acoustic properties

By displacing the measurement cell in the acoustic field, it is possible to map the acoustic properties of the gel. However, the cell presented in section II C 1 had only a small window (in order to ensure temperature control) which did not allow for scanning a representative field of the sample. In order to check the homogeneity of acoustic properties of the Ludox gel, we scanned a sample formulated in a cell culture flask (which has the interest to offer large, flat and homogeneous sides) that was left to age for about 10h in order to reach a stationary state and sealed with Parafilm to minimize evaporation. There was thus no control of the temperature in this experiment: the cell was in a water bath to ensure acoustic propagation, but it followed room temperature fluctuations.

We scanned a field of 1.4 cm in height and 3.2 cm in width, by steps of 1 mm corresponding to a map of about 450 points: such a scan takes about 2h. These steps are small compared to the acoustic beam (of radius of about 3 mm): there is thus a correlation between successive points. The cell was moved in successive vertical columns in order to avoid possible vertical temperature gradient due to the partial withdrawal of the cell from the bath when moving it up. Resulting maps of average acoustic speed and attenuation are displayed on Fig. 10.

First, we observe an apparent lateral gradient of acoustic velocity. This is most probably be due to room temperature variations which are likely on the time scale of the experiment, as there is no reason to observe such a regular gradient orthogonal to gravity. Temperature has however a smaller impact on acoustic attenuation, as can be seen by the absence of overall tendency in acoustic maps: we can consequently still exploit these, at least qualitatively.

We mapped different samples and the result presented in Fig. 10(b) is representative: the gel displays some spots

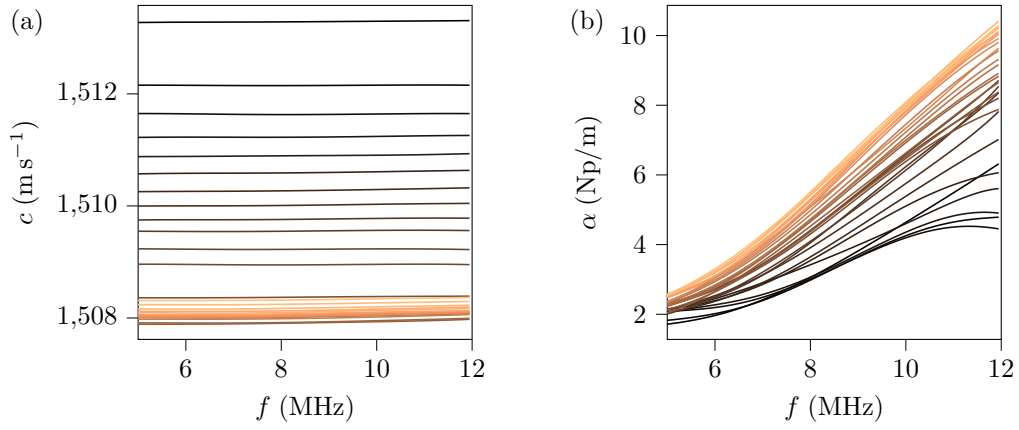


FIG. 7. Evolution of sound speed (a) and attenuation (b) spectra over time (lighter colors correspond to longer times, curves are spaced regularly by 4 min) for a gel of particle volume fraction $\phi = 5.9\%$ and salt concentration $[\text{NaCl}] = 0.55 \text{ molL}^{-1}$.

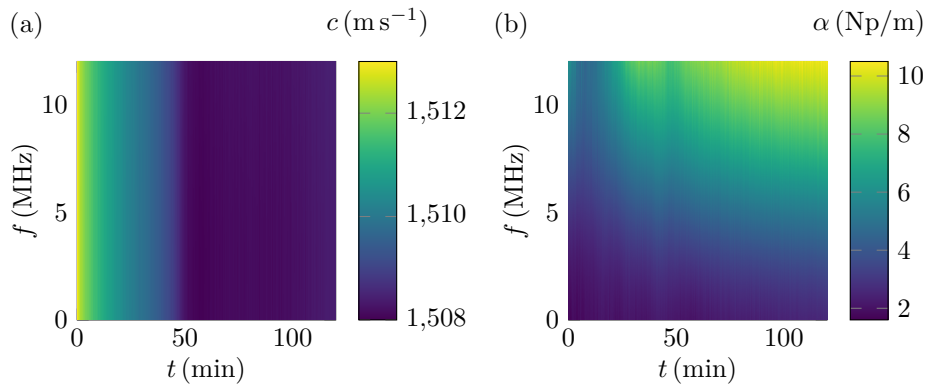


FIG. 8. Time-frequency representation of the acoustic speed (a) and attenuation (b) spectra during the gelation of a sample of volume fraction $\phi = 5.9\%$ and salt concentration $[\text{NaCl}] = 0.55 \text{ molL}^{-1}$. Note that the variations of sound speed are very small.

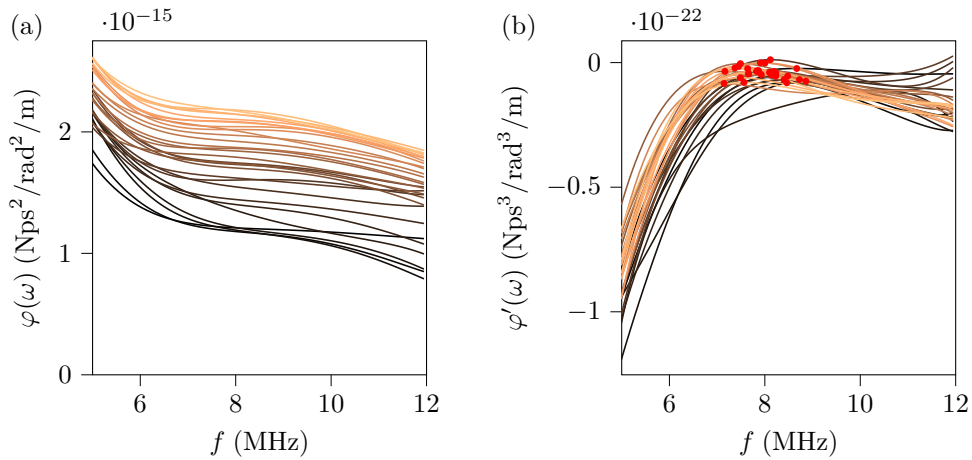


FIG. 9. Representation of reduced attenuation $\varphi(\omega) = \alpha/\omega^2$ (a) and its derivative (b) as a function of frequency at different times of the gelation of a sample of volume fraction $\phi = 5.9\%$ and salt concentration $[\text{NaCl}] = 0.55 \text{ molL}^{-1}$. Lighter colors correspond to longer times, and curves are regularly spaced by 4 min. On curve (b), the red dots are the identified maximum corresponding to an inflection of φ and to an inverse typical relaxation time.

with higher attenuation in a rather homogeneous background.

Without further study, it is uneasy to determine the cause of

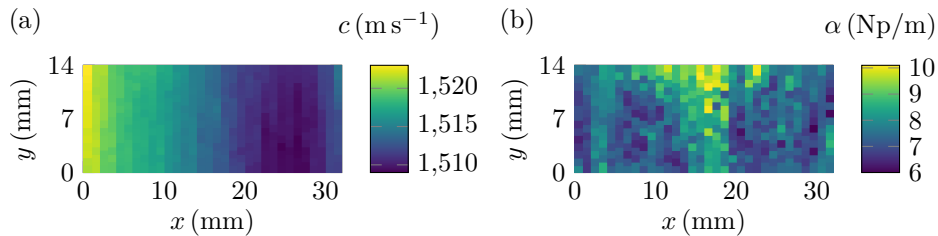


FIG. 10. Map of average sound speed (a) and attenuation (b) of a gel with brine concentration $[\text{NaCl}] = 0.55 \text{ molL}^{-1}$. The sample was left to age for about 10h before measurement was performed, so that it can be considered as almost stationary.

these heterogeneities: they could for instance be due to intrinsically heterogeneous gelation, to imperfect initial mixing of the solutions or to the possible trapping of air bubbles. They could explain the variability of absolute values of attenuation from sample to sample. However, this does not compromise our comparative results of samples at different concentrations. These heterogeneities are indeed localized and outside of these zones, attenuation is rather homogeneous: the relative standard deviation of attenuation is $(\sigma_\alpha / \langle \alpha \rangle) \simeq 10\%$. Consequently, provided that the acoustic path crosses an homogeneous part of the sample, these fluctuations remain small enough to discriminate between the different concentrations on Fig. 5.

V. CONCLUSION AND PERSPECTIVES

In this paper, we presented a simple setup to measure acoustic sound and attenuation spectra by a pulse-echo method in order to monitor the evolution of physico-chemical processes. As a proof of principle, we used it to characterize the kinetics of gelation of a colloidal silica suspension after destabilization by mixing with a brine: despite being a well known system for studies on gelation, this had not yet been characterized acoustically. We showed that sound attenuation allows us to define a typical time for the system evolution which is proportional to gelation times that are obtained from conventional rheometrical measurements. This opens interesting path for the study of gelation in industrial context, in systems where optical access is not possible: in particular, our setup can be easily adapted for an inline characterization of industrial processes and use of focused transducer makes it applicable to small volumes.

We attempted to exploit in more details the full acoustic spectra: while sound speed displays no significant dispersion, it appears that attenuation contains interesting information on the gel. The overall attenuation evolves quadratically in frequency, as expected from a simple viscoelastic modeling. However, deviations from this scaling suggests the existence of a relaxation phenomenon, characterized by a typical time that does not evolve during the gelation process and is similar for the different salt concentrations of the gel. As often in acoustic spectroscopy, it is however hard to obtain definitive conclusions as various models can fit satisfactorily with measurements, and a detailed analysis of mechanisms of sound attenuation is required together with measurements on a wider

frequency range.

Finally, our setup allows to perform mappings of the acoustic properties of the sample. At the current stage, the results remain very qualitative due to biases caused by the lack of temperature control and to the poor spatial and temporal resolution. It however shows that the gels under study here are mostly homogeneous but have areas with significant acoustic contrast: this could explain the mediocre reproducibility of the absolute values of attenuation but does not compromise our conclusions on gelation time. An improved setup, with a cell of controlled temperature with a wide window, focused transducers, enlarged frequency range and higher scanning speed, would allow us to monitor the gelation in both space and time, which is also interesting for characterization of industrial systems.

Our work shows that acoustic spectroscopy offers great opportunities for the characterization of soft materials. Further work will improve the current setup and focus on other systems, and implement the experiment on inline industrial processes.

ACKNOWLEDGMENTS

We thank the Région Nouvelle-Aquitaine for funding through the HoloFluid-3D project and Solvay for funding NB PhD. We are grateful to Dr. Thomas Brunet for interesting discussions about our setup and results. We also thank Pr. Sébastien Manneville and Dr. Thomas Gibaud for suggestions on Ludox gels formulation. We finally thank Dr. Valentin Leroy for bringing interesting references to our knowledge.

Appendix A: Details on acoustic signal analysis

In this appendix, we provide the reader with more details on the treatment of acoustic signal to retrieve quantities of interest. All signal analysis is coded in Python and uses libraries Numpy, SciPy and Pandas.

1. Analysis of a acoustic signal

Figure 11 shows the different steps to isolate a single peak on a given signal. Figure (a) presents an example of signal

observed in transmission, with two successive pulses corresponding to different trajectories in the sample: in order to further analyze the signal, it is necessary to separate these echoes. The cell is built such that there is no overlap between the different echoes, which simplifies the procedure. It is to note that the signal is actually averaged over 10 successive excitations of the emitting transducer in order to improve the signal to noise ratio. We then extract the envelope of the signal by taking its analytical part, using Hilbert transform (Fig. (b)): by applying a simple threshold, we finally determine the support of the different echoes (Fig. (c)) which allows to separate them from each other.

An example of signal and its spectrum is displayed on Fig. 12.

2. Calibration procedure and measurement of sound speed and attenuation

When the different echoes of the signals measured on the two transducers are isolated, we compute their Fourier transforms. In order to measure the excess time of flight and attenuation of the sample with respect to water, we need to consider:

- the signal $u_{a,r}$ obtained after a single reflection on the cell filled with air,
- the signal $u_{w,r}$ obtained after a single reflection on the cell filled with water,
- the signal $u_{w,t}$ obtained after direct transmission through the cell filled with water,
- the signal $u_{s,r}$ obtained after a single reflection on the cell filled with the sample,
- the signal $u_{s,t}$ obtained after direct transmission through the cell filled with the sample.

We denote by u^0 the spectral content of the acoustic wave initially generated by the emitting transducer. All the quantities in this section depend on frequency but we do not write it for the sake of simplicity. We denote by $r_{1/2}$ and $t_{1/2} = 1 + r_{1/2}$ the reflection and transmission coefficient in amplitude for a

wave arriving on an interface between two media (1) and (2) from medium (1), and we have $r_{1/2} = -r_{2/1}$ [63]. Here, the different possible media are water (w), air (a), polycarbonate window (PC) and the sample under study (s). We finally denote by ℓ the cell thickness.

By writing the phase and attenuation due to propagation and the coefficients associated with reflection and transmission through interfaces for the different signals, and by assuming that the interface between the polycarbonate window and air is an ideal reflector ($r_{PC/a} = 1$), we can calibrate the experiment and retrieve the quantities we are interested in. First, by considering the ratio between the reflection on air and on the sample, and on air and on water, we respectively obtain the reflection coefficients on the window:

$$r_{w/PC} = \frac{u_{w,r}}{u_{a,r}} \text{ and } r_{s/PC} = \frac{u_{s,r}}{u_{a,r}}. \quad (\text{A1})$$

From these coefficients, we can also easily deduce the associated transmission coefficients. Knowing these factors, the excess attenuation and time of flight in sample with respect to water can be obtained by normalizing the transmitted signal through the sample and through the water:

$$\alpha_s - \alpha_w = \frac{1}{\ell} \ln \left| \frac{1 - r_{s/PC}^2}{1 - r_{w/PC}^2} \frac{u_{w,t}}{u_{s,t}} \right| \quad (\text{A2})$$

and:

$$\frac{\ell}{c_s} - \frac{\ell}{c_w} = \frac{1}{\omega \arg \left[\frac{1 - r_{s/PC}^2}{1 - r_{w/PC}^2} \right]} \left[\arg \left(\frac{u_{s,t}}{u_{w,t}} \right) + 2q\pi \right] \quad (\text{A3})$$

where q is an integer. This parameter is due to the fact that the phase is known modulo 2π . In order to measure it, we unwrap the phase of $u_{s,t}/u_{w,t}$ which is almost linear with frequency, and extrapolate it at null frequency, giving a value $-A$. The physical phase difference between the two signals should cancel in this limit, so we take q as the floor of A .

Attenuation α_w and sound speed c_w in water are taken from reference values [48, 49]. Finally, ℓ is obtained by measuring the difference of time of flight for a cell filled with water between the reflection at the first window/water interface (corresponding to signal $u_{w,r}$) and at the water/second window interface.

[1] J. Bercoff, M. Tanter, and M. Fink, "Supersonic shear imaging: A new technique for soft tissue elasticity mapping," *IEEE transactions on ultrasonics, ferroelectrics, and frequency control* **51**, 396–409 (2004).

[2] C. Errico, J. Pierre, S. Pezet, Y. Desailly, Z. Lenkei, O. Couture, and M. Tanter, "Ultrafast ultrasound localization microscopy for deep super-resolution vascular imaging," *Nature* **527**, 499–507 (2015).

[3] J. Wiklund, I. Shahram, and M. Stading, "Methodology for in-line rheology by ultrasound doppler velocity profiling and pressure difference techniques," *Chemical Engineering Science* **62**, 4277–4293 (2007).

[4] T. Gallot, C. Perge, V. Grenard, M. Fardin, N. Taberlet, and

S. Manneville, "Ultrafast ultrasonic imaging coupled to rheometry: Principle and illustration," *Review of Scientific Instruments* **84**, 045107 (2013).

[5] J. Markham, R. Beyer, and R. Lindsay, "Absorption of sound in fluids," *Reviews of Modern Physics* **23**, 353–411 (1951).

[6] N. Hirai and H. Eyring, "Bulk viscosity of liquids," *Journal of Applied Physics* **29**, 810–816 (1958).

[7] D. Laux, M. Valente, J. Ferrandis, N. Talha, O. Gibert, and A. Prades, "Shear viscosity investigation on mango juice with high frequency longitudinal ultrasonic waves and rotational viscosimetry," *Food Biophysics* **8**, 233–239 (2013).

[8] D. Laux, O. Gibert, J. Ferrandis, M. Valente, and A. Prades, "Ultrasonic evaluation of coconut water shear viscosity," *Jour-*

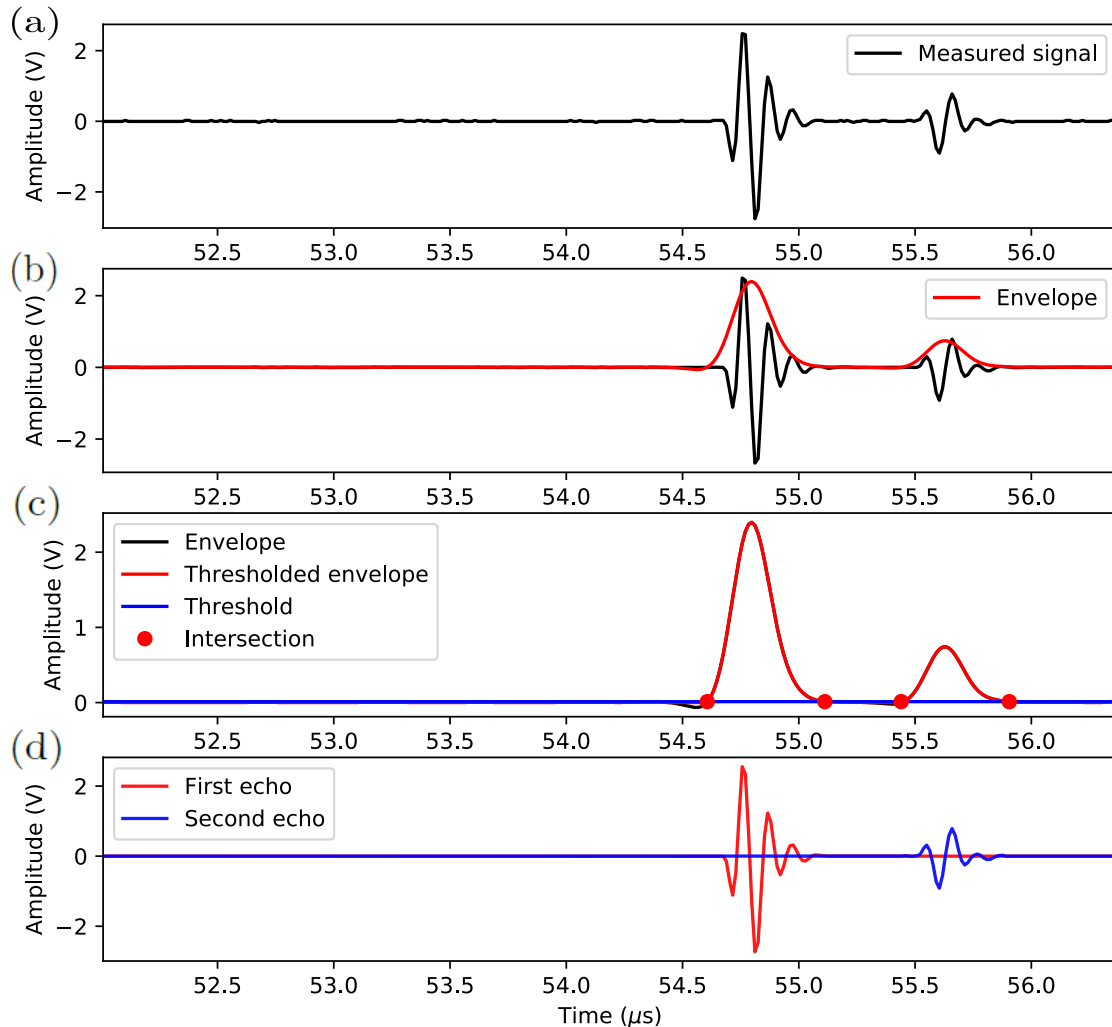


FIG. 11. Illustration of the method used to isolate echoes on a signal, for a measurement in reflection mode. The initial signal (a) shows two echoes corresponding to the reflections at the two interfaces of the window. The envelope of the signal is extracted by taking its analytical part. The obtained envelope is then thresholded to retrieve the times at which a given echo starts and stops (c). The isolated echoes are highlighted in different colors (d).

- nal of Food Engineering **126**, 62–64 (2014).
- [9] E. Franco and F. Buiocchi, “Ultrasonic measurement of viscosity: Signal processing methodologies,” *Ultrasonics* **91**, 213–219 (2019).
- [10] P. Longin, C. Verdier, and M. Piau, “Dynamic shear rheology of high molecular weight polydimethylsiloxanes: comparison of rheometry and ultrasound,” *Journal of Non-Newtonian Fluid Mechanics* **76**, 213–232 (1998).
- [11] C. Verdier, P. Longin, and M. Piau, “Dynamic shear and compressional behavior of polydimethylsiloxanes: Ultrasonic and low frequency characterization,” *Rheologica Acta* **37**, 234–244 (1998).
- [12] V. Leroy, K. Pitura, M. Scanlon, and J. Page, “The complex shear modulus of dough over a wide frequency range,” *Journal of Non-Newtonian Fluid Mechanics* **165**, 475–478 (2010).
- [13] M. Scanlon and J. Page, “Probing the properties of dough with low-intensity ultrasound,” *Cereal Chemistry* **92**, 121–133 (2015).
- [14] G. Lefebvre, R. Wunenburger, and T. Valier-Brasier, “Ultrasonic rheology of visco-elastic materials using shear and longitudinal waves,” *Applied Physics Letters* **112**, 241906 (2018).
- [15] F. Eggers and U. Kaatze, “Broad-band ultrasonic measurement techniques for liquids,” *Measurement Science and Technology* **7**, 1–19 (1996).
- [16] U. Kaatze, T. Hushcha, and F. Eggers, “Broad-band ultrasonic measurement techniques for liquids,” *Journal of Solution Chemistry* **29**, 299–368 (2000).
- [17] D. Forrester, J. Huang, and V. Pinfield, “Characterisation of colloidal dispersions using ultrasound spectroscopy and multiple-scattering theory inclusive of shear-wave effects,” *Chemical Engineering Research and Design* **114**, 69–78 (2016).
- [18] D. Forrester, J. Huang, V. Pinfield, and F. Luppé, “Experimental verification of nanofluid shear-wave reconversion in ultrasonic fields,” *Nanoscale* **8**, 84–88 (2016).
- [19] H. Mori, T. Norisuye, H. Nakanishi, and Q. Tran-Cong-Miyata, “Ultrasound attenuation and phase velocity of micrometer-sized

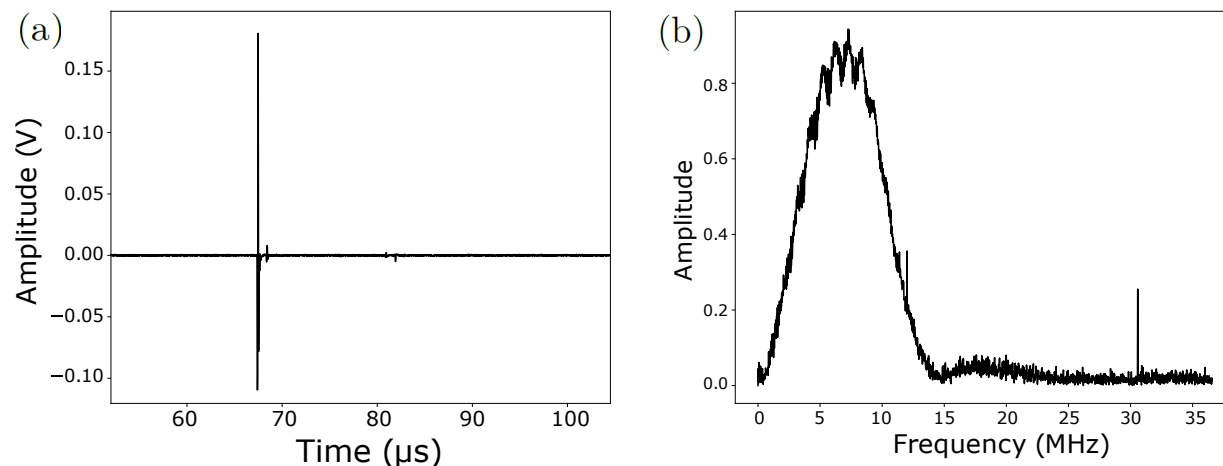


FIG. 12. Example of acoustic signal (in transmission) (a) and of its intensity spectrum (b).

particlesuspensions with viscous and thermal losses,” *Ultrasonics* **83**, 171–178 (2018).

- [20] P. Epstein and R. Carhart, “The absorption of sound in suspensions and emulsions. i. water fog in air,” *Journal of the Acoustical Society of America* **25**, 553–565 (1953).
- [21] J. Allegra and S. Hawley, “Attenuation of sound in suspensions and emulsions: Theory and experiments,” *Journal of the Acoustical Society of America* **51**, 1545–1564 (1972).
- [22] R. Challis, M. Povey, M. Mather, and A. Holmes, “Ultrasound techniques for characterizing colloidal dispersions,” *Reports on Progress in Physics* **68**, 1541–1637 (2005).
- [23] R. Al-Lashi and R. Challis, “Effective viscosity in a wave propagation model for ultrasonic particle sizing in non-dilute suspensions,” *Journal of the Acoustical Society of America* **136**, 1583–1890 (2014).
- [24] V. Pinfield, D. Forrester, and F. Luppé, “Ultrasound propagation in concentrated suspensions: shear-mediated contributions to multiple scattering,” *Physics Procedia* **70**, 213–216 (2015).
- [25] T. Valier-Brasier, J. Conoir, F. Coulouvrat, and J. Thomas, “Sound propagation in dilute suspensions of spheres: Analytical comparison between coupled phase model and multiple scattering theory,” *Journal of the Acoustical Society of America* **138**, 2598–2612 (2015).
- [26] D. Forrester, J. Huang, and V. Pinfield, “Modelling viscous boundary layer dissipation effects in liquid surrounding individual solid nano and micro-particles in an ultrasonic field,” *Scientific Reports* **9**, 4956 (2019).
- [27] A. Dukhin and P. Goetz, “Acoustic spectroscopy for concentrated polydisperse colloids with high density contrast,” *Langmuir* **12**, 4987–4997 (1996).
- [28] A. Dukhin and P. Goetz, *Characterization of Liquids, Nano- and Microparticulates, and Porous Bodies using Ultrasound* (Elsevier, 2010).
- [29] L. Landini and R. Sarnelli, “Evaluation of the attenuation coefficients in normal and pathological breast tissue,” *Medical & Biological Engineering & Computing* **24**, 243–247 (1986).
- [30] H. Jongen, J. Thijssen, M. van den Aarssen, and W. Verhoef, “A general model for the absorption of ultrasound by biological tissues and experimental verification,” *Journal of the Acoustical Society of America* **79**, 535–540 (1986).
- [31] K. Parker, M. Asztely, R. Lerner, E. Schenk, and R. Waag, “In-vivo measurements of ultrasound attenuation in normal or diseased liver,” *Ultrasound in Medicine & Biology* **14**, 127–136 (1988).
- [32] G. Bonacucina, M. Misici-Falzi, M. Cespi, and G. Palmieri, “Characterization of micellar systems by the use of acoustic spectroscopy,” *Journal of Pharmaceutical Sciences* **97**, 2217–2227 (2008).
- [33] G. Bonacucina, D. Perinelli, M. Cespi, L. Casettari, R. Cossi, P. Blasi, and G. Palmieri, “Acoustic spectroscopy: A powerful analytical method for the pharmaceutical field?” *International Journal of Pharmaceutics* **50**, 174–195 (2016).
- [34] R. Giordano, F. Mallamace, and F. Wanderlingh, “Acoustic absorption and thixotropic structure in lysozyme solution,” *Il Nuovo Cimento* **2D**, 1272–1280 (1983).
- [35] D. Dagleish, E. Verespej, M. Alexander, and M. Corredig, “The ultrasonic properties of skim milk related to the release of calcium from casein micelles during acidification,” *International Dairy Journal* **15**, 1105–1112 (2005).
- [36] P. Resa, L. Elvira, F. Montero de Espinosa, R. González, and J. Barcenilla, “On-line ultrasonic velocity monitoring of alcoholic fermentation kinetics,” *Bioprocess and Biosystems Engineering* **32**, 321–331 (2009).
- [37] M. Derra, F. Bakkali, A. Amghar, and H. Sahseh, “Estimation of coagulation time in cheese manufacture using an ultrasonic pulse-echo technique,” *Journal of Food Engineering* **216**, 65–71 (2018).
- [38] P. Griesmar, A. Ponton, S. Serfaty, B. Senouci, M. Gindre, G. Gouedard, and S. Warlus, “Kinetic study of silicon alkoxides gelation by acoustic and rheology investigations,” *Journal of Non-Crystalline Solids* **319**, 57–64 (2003).
- [39] W. Krasaekoopt, B. Bhandari, and H. Deeth, “Comparison of gelation profile of yoghurts during fermentation measured by rva and ultrasonic spectroscopy,” *International Journal of Food Properties* **8**, 193–198 (2005).
- [40] N. Parker and M. Povey, “Ultrasonic study of the gelation of gelatin: Phase diagram, hysteresis and kinetics,” *Food Hydrocolloids* **26**, 99–107 (2012).
- [41] S. Serfaty, P. Griesmar, M. Gindre, G. Gouedard, and P. Figure, “An acoustic technique for investigating the sol–gel transition,” *Journal of Materials Chemistry* **8**, 2229–2231 (1998).
- [42] J. Trompette and M. Meireles, “Ion-specific effect on the gelation kinetics of concentrated colloidal silica suspensions,” *Journal of Colloid and Interface Science* **263**, 522–527 (2003).
- [43] J. Trompette and M. Clifton, “Influence of ionic specificity on the microstructure and the strength of gelled colloidal silica sus-

- pensions,” *Journal of Colloid and Interface Science* **276**, 475–482 (2004).
- [44] X. Cao, H. Cummins, and J. Morris, “Structural and rheological evolution of silica nanoparticle gels,” *Soft Matter* **6**, 5425–5433 (2010).
- [45] J. Trompette and C. Bordes, “Rheological study of the gelation kinetics of a concentrated latex suspension in the presence of nonadsorbing polymer chains,” *Langmuir* **16**, 9627–9633 (2000).
- [46] J. Trompette, “Influence of co-ion nature on the gelation kinetics of colloidal silica suspensions,” *Journal of Physical Chemistry B* **121**, 5654–5659 (2017).
- [47] Y. Hallez and M. Meireles, “Fast, robust evaluation of the equation of state of suspensions of charge-stabilized colloidal spheres,” *Langmuir* **33**, 10051–10060 (2017).
- [48] W. Marczak, “Water as a standard in the measurements of speed of sound in liquids,” *Journal of the Acoustical Society of America* **102**, 2776–2779 (1997).
- [49] M. Holmes, N. Parker, and M. Povey, “Temperature dependence of bulk viscosity in water using acoustic spectroscopy,” *Journal of Physics: Conference Series* **269**, 012011 (2011).
- [50] H. Winter, “Can the gel point of a cross-linking polymer be detected by the $g' - g''$ crossover?” *Polymer Engineering and Science* **27**, 1698–1702 (1987).
- [51] F. Chambon and H. Winter, “Linear viscoelasticity at the gel point of a crosslinking pdms with imbalanced stoichiometry,” *Journal of Rheology* **31**, 683–697 (1987).
- [52] E. Holly, S. Venkataraman, F. Chambon, and H. Winter, “Fourier transform mechanical spectroscopy of viscoelastic materials with transient structure,” *Journal of Non-Newtonian Fluid Mechanics* **27**, 17–26 (1988).
- [53] D. Hodgson and E. Amis, “Dynamic viscoelastic characterization of sol-gel reactions,” *Macromolecules* **23**, 2512–2519 (1990).
- [54] H. Winter, “Polymer gels, materials that combine liquid and solid properties,” *MRS Bulletin*, 44–48 (1991).
- [55] E. Drabarek, J. Bartlett, H. Hanley, J. Woolfrey, and C. Muzny, “Effect of processing variables on the structural evolution of silica gels,” *International Journal of Thermophysics* **23**, 145–160 (2002).
- [56] T. Matsunaga and M. Shibayama, “Gel point determination of gelatin hydrogels by dynamic light scattering and rheological measurements,” *Physical Review E* **76**, 030401 (2021).
- [57] T. Gibaud, N. Dagès, P. Lidon, G. Jung, L. Ahouré, M. Sztucki, A. Poulesquen, N. Hengl, F. Pignon, and S. Manneville, “Rheoacoustic gels: Tuning mechanical and flow properties of colloidal gels with ultrasonic vibrations,” *Physical Review X* **10**, 011028 (2020).
- [58] T. Szabo and J. Wu, “A model for longitudinal and shear wave propagation in viscoelastic media,” *Journal of the Acoustical Society of America* **107**, 2437–2446 (2000).
- [59] C. Bryant and D. McClements, “Ultrasonic spectroscopy study of relaxation and scattering in whey protein solutions,” *Journal of the Science of Food and Agriculture* **79**, 1754–1760 (1999).
- [60] V. Shilov, V. Sperkach, Y. Sperkach, and A. Strybulevych, “Acoustic relaxation of liquid poly(tetramethylene oxide) with hydroxyl and acyl terminal groups,” *Polymer Journal* **34**, 565–574 (2002).
- [61] N. Jiménez, F. Camarena, J. Redondo, V. Sánchez-Morcillo, Y. Hou, and E. Konofagou, “Time-domain simulation of ultrasound propagation in a tissue-like medium based on the resolution of the nonlinear acoustic constitutive relations,” *Acta Acustica* **102**, 876–892 (2016).
- [62] D. Holmes, J. Lee, H. Park, and M. Pezulla, “Nonlinear buckling behavior of a complete spherical shell under uniform external pressure and homogenous natural curvature,” *Physical Review E* **102**, 023003 (2020).
- [63] L. Kinsler, A. Frey, A. Coppens, and J. Sanders, *Fundamentals of Acoustics* (Wiley, 2000).